Electronic Supplementary Information

Hydrogen bonding boosted persistent room temperature phosphorescence of pure organics for multiple applications

Tingting Zhang,[a,b] Heqi Gao,[c] Anqi Lv,[d] Ziyi Wang,[e] Yongyang Gong,[f] Dan Ding,[c] Huili Ma,*[d]

Yongming Zhang*[a,b] and Wang Zhang Yuan*[b]

[a] School of Materials Science and Engineering, Shanghai Jiao Tong University, 800 Dongchuan Road, Shanghai 200240, China.

[b] Shanghai Key Lab of Electrical Insulation and Thermal Aging, School of Chemistry and Chemical Engineering, Shanghai Jiao Tong University, 800 Dongchuan Road, Shanghai 200240, China. E-mail: ymzhang@sjtu.edu.cn (Y.Z.), wzhyuan@sjtu.edu.cn (W.Z.Y.).

[c] State Key Laboratory of Medicinal Chemical Biology, Key Laboratory of Bioactive Materials, Ministry of Education, College of Life Sciences, Nankai University, Tianjin 300071, China.

[d] Key Laboratory of Flexible Electronics (KLOFE) & Institute of Advanced Materials (IAM), Nanjing Tech University, 30 South Puzhu Road, Nanjing 211816, China. E-mail: iamhlma@njtech.edu.cn (H.M).

[e] Department of Materials Science and Engineering, Northwestern University, Evanston, Illinois 60208, United State.

[f] Key Laboratory of New Processing Technology for Non-ferrous Metals and Materials, Ministry of Education, Guangxi Key Laboratory of New Energy and Building Energy Saving, College of Materials Science and Engineering, Guilin University of Technology, Guilin 541004, China.

Experimental Section

Instruments. Emission and UV-vis absorption spectra were respectively tested on a LS 55 (Perkin Elmer Inc., USA) fluorescence spectrometer and an ultraviolet/visible light photometer Lambda 35 (Perkin Elmer, Inc., USA). With a delay time (t_d) of ≥ 0.1 ms, all nanosecond emission signals can be excluded according to the fluorescence spectrometer instructions. ^{1}H NMR and ^{13}C NMR data were recorded on a AVANCE III HD 500 NMR spectrometer in deuterated dimethylsulfoxide (DMSO-d_6) at room temperature, and chemical shifts were reported in ppm relative to tetramethylsilane (TMS, $\delta = 0$ ppm). Absolute emission efficiencies (Φ_c) and fluorescence lifetimes ($<\tau>_f$) of crystals, films and solutions were determined on a QM/TM/IM steady-transient time-resolved spectroscopy (PTI, USA). Emission lifetimes of the crystalline samples were measured on a FLS980 (Edinburgh, UK) spectrofluorometer. XRD data was recorded on a D8 Advance diffractometer (Bruker, German) at a scan rate of 6° (2θ)/min (scan range: 2-70°). Single crystal data was recorded on a Bruker D8 VENTURE CMOS photon 100 diffractometer with helios mx multilayer monochromator Cu with Kα radiation (λ = 1.54178 Å). High resolution mass spectra (HRMS) were performed on an ultra-high performance liquid chromatography-quadrupole time-of-flight mass spectrometer (ACQUITYTM UPLC & Q-TOF MS Premier, USA). Photographs and video were taken on a digital camera (Canon EOS 70D, Japan). Dynamic light scattering (DLS) was performed on a 90 plus particle size analyzer. In vitro and in vivo afterglow imaging were collected on IVIS Lumina II imaging system.

Materials. Methyl 4-bromobenzoate (Energy Chemical Ltd.), methyl 3-bromobenzoate (J&K Chemical Scientific Ltd.), methyl 2-bromobenzoate (J&K Chemical Scientific Ltd.), palladium acetate [$Pd(OAc)_2$, J&K Chemical Scientific Ltd.], tri-tert-butylphosphine [P(t-Bu)$_3$, Adamas Reagent Ltd.] polymethyl methacrylate (PMMA) (TCI Shanghai Development Co., Ltd.) and carbazole (CZ, Adamas

Reagent Ltd.) were analytical reagents. CZ was purified through column chromatography before use, and other materials were used directly. Sodiumhydroxide, tetrahydrofuran (THF), methanol, hydrochloric acid (concentration = 35%), 1,2-dichloroethane, petroleum ether (PE), toluene and copper powder were obtained from Sinopharm Chemical Reagent Co. Ltd. and used as received. The amphiphilic surfactant PEG-*b*-PPG-*b*-PEG (F127) was purchased from Laysan Bio, Inc. (Arab, AL).

Synthesis of 4-BACZ, 3-BACZ and 2-BACZ. We synthesized methyl 4-(9H-carbazol-9-yl)benzoate (4-MBACZ), methyl 3-(9H-carbazol-9-yl)benzoate (3-MABCZ) and methyl 2-(9H-carbazol-9-yl)benzoate (2-MBACZ) using carbazole (CZ) and methyl benzoate (MBA) conjugates in our previous report [S1]. In this paper, we further synthesized the corresponding acids as below route.[S2] 4-(9H-carbazol-9-yl)benzoic acid (4-BACZ) was synthesized first as route below. 4-MBACZ (347.3 mg) was dissolved in tetrahydrofuran (10 mL) in a two-neck flask, and 5 mL methanol was added, followed by 5 mL sodium hydroxide solution (0.8 M). The reaction was started under 55 ^{o}C overnight, and the reaction was confirmed to be end through thin-layer chromatography (TLC). The reaction mixture was then poured into a beaker containing deionized water (500 mL) and hydrochloric acid (concentration 35%, 10 mL), then white precipitate was obtained. After standing for 5 h, the white precipitate was filtered and dried in a vacuum oven, then white solid (320.8 mg) was obtained in yield 96.9%. ^{1}H NMR (500 MHz, DMSO-d_6, δ, ppm) of 4-BACZ: 13.17 (s, 1H), 8.26-8.22 (m, 4H), 7.79-7.77 (m, 2H), 7.50-7.45 (m, 4H), 7.33-7.30 (m, 2H); ^{13}C NMR (126 MHz, DMSO-d_6, δ, ppm) of 4-BACZ: 166.69, 140.84, 139.58, 131.27, 129.37, 126.42, 126.27, 123.09, 120.59, 120.54, 109.77. HRMS, $[M+H]^+$: calcd. 288.1025, found 288.1020.

3-(9H-carbazol-9-yl)benzoic acid (3-BACZ) and 2-(9H-carbazol-9-yl)benzoic acid (2-BACZ) were synthesized in similar approach in yields 94.0% and 84.3% respectively. ^{1}H NMR (500 MHz, DMSO-

d_6, δ, ppm) of 3-BACZ: 13.33 (s, 1H), 8.27-8.26 (d, 2H), 8.11-8.10 (t, 2H), 7.93-7.91 (d, 1H), 7,84-7.83 (t, 1H), 7.45-7.39 (m, 4H), 7.33-7.30 (t, 2H). ^{13}C NMR (126 MHz, DMSO-d_6, δ, ppm) of 3-BACZ: 167.06, 140.43, 137.64, 133.33, 131.55, 131.18, 128.79, 127.52, 126.87, 123.34, 121.10, 120.80, 109.93. HRMS, $[M+H]^+$: calcd. 288.1025, found 288.1018.

^{1}H NMR (500 MHz, DMSO-d_6, δ, ppm) of 2-BACZ: 12.65 (s, 1H), 8.23-8.22 (d, 2H), 8.09-8.07 (m, 1H), 7.86-7.84 (m, 1H), 7.73-7.69 (m, 1H), 7.63 -7.62 (m, 1H), 7.39-7.38 (m, 2H), 7.27-7.26 (m, 2H), 7.10-7.08 (d, 2H). ^{13}C NMR (126 MHz, DMSO-d_6, δ, ppm) of 2-BACZ: 166.70, 141.01, 135.52, 133.38, 131.33, 131.12, 129.88, 128.73, 126.01, 122.62, 120.35, 119.56, 109.24. HRMS, $[M+H]^+$: calcd. 288.1025, found 288.1024.

Crystal culture. Single crystals of 4-BACZ, 3-BACZ and 2-BACZ, which are suitable for X-ray crystallography, were obtained through slow evaporation from their dilute solution in chloroform.

Computational Details. The 4-BACZ, 3-BACZ, 2-BACZ molecules were extracted from their crystal structures, the 4-MBACZ, 3-BMACZ, 2-MBACZ molecules were extracted from the crystal structures in report [S1]. The computational models were built from the crystal structure. The quantum mechanics/molecular mechanics (QM/MM) theory with two-layer ONIOM method was implemented to deal with the electronic structures in crystal, where the central molecule is chosen as the active QM part and set as the high layer, while the surrounding ones are chosen as the MM part and defined as the low layer. The universal force field (UFF) was used for the MM part, and the molecules of MM part were frozen during the QM/MM geometry optimizations. The electronic embedding is adopted in QM/MM calculations by incorporating the partial charges of the MM region into the quantum

mechanical Hamiltonian. The B3LYP/6-31G(d) was employed to evaluate the natural transition orbitals (NTOs) for the lowest triplet states and reorganization energy by using Gaussian 09 package.[S3]

Preparation of films. After the sample (4-BACZ/3-BACZ/2-BACZ) (1 mg) and PMMA (99 mg) were dissolved in 1,2-dichloroethane (5 mL), a piece of transparent film was obtained by drop casting and dried in a vacuum oven at 40 ^{o}C for overnight before use.

Preparation of nanoparticles (NPs). The sample 4-BACZ, 3-BACZ or 2-BACZ solids (1 mg) was added into the aqueous solution (3 mL) of F127 (10 mg). The solution was then sonicated for 10 minutes through a microtip-equipped probe sonicator (Branson, S-250D). Afterwards, NPs solution was obtained by filtering the mixture in a 0.45 μm syringe driven filter.

Cell Culture. We purchased Hela cervical cancer cells from American Type Culture Collection (ATCC). The cells were cultured with 1% penicillin-streptomyc and 10% FBS in Dulbecco's Modified Eagle Medium (DMEM).

Cytotoxicity Study. Cytotoxicity tests were conducted according to the 3-(4,5-dimethylthiazol-2-yl)-2,5-diphenyl tetrazolium bromide (MTT) assay. A 96-well plates (Costar, IL, USA) contained sample NPs of concentration 25, 50, 100 and 200 μM respectively. Hela cancer cells were seeded and kept at 37 ^{o}C for 48 h, then washed twice with 1×PBS. 100 μL of freshly prepared MTT (0.5 mg/mL) solution was added for each well. 3 h later, after removing the MTT solution, DMSO (100 μL) was added into each well. The plate was then gently shaken for 10 minutes. Cell viability was expressed. The ratio was of the absorbance of cells cultured in NPs suspension to that of cells cultured only in medium reflects cell viability. The absorbance of cells was tested on the microplate reader (Genios Tecan).

In Vivo Afterglow Imaging. We purchased BALB/c nude mice aged at 6 weeks from the Laboratory

Animal Center of the Academy of Military Medical Sciences (Beijing, China) in this paper.

After being anesthetized with 2% isoflurane at oxygen atmosphere, the nude mice were subcutaneously injected the sample NPs (25 nM based on NPs) at the left back, then placed in IVIS instrument cabinet, and subjected to 30 s irradiation with a hand-held UV lamp (10 mW cm^{-2}) at 365 nm. Then, in the bioluminescence mode, the IVIS system was used to remove the light source, and an open filter (exposure time: 17 s) was set to obtain the image. During this process, the mice were placed on a heating pad.

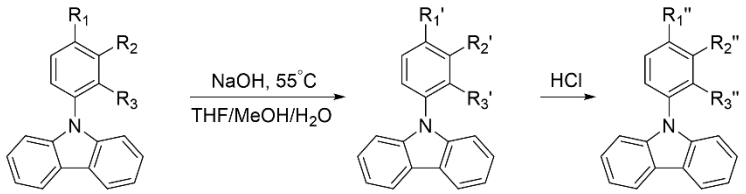

R_2 = R_3 = H, R_1 = $COOCH_3$, 4-MBACZ
R_1 = R_3 = H, R_2 = $COOCH_3$, 3-MBACZ
R_1 = R_2 = H, R_3 = $COOCH_3$, 2-MBACZ

R_2" = R_3" = H, R_1" = H, 4-BACZ
R_1" = R_3" = H, R_2" = H, 3-BACZ
R_1" = R_2" = H, R_3" = H, 2-BACZ

Scheme S1 Synthetic route to 4-BACZ, 3-BACZ and 2-BACZ.

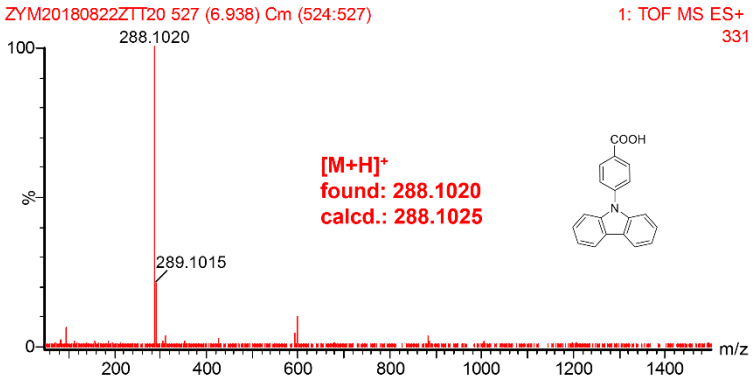

Fig. S1 High resolution mass spectrum of 4-BACZ.

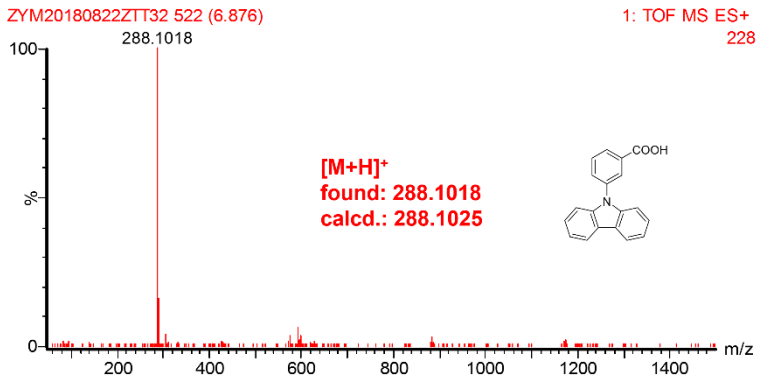

Fig. S2 High resolution mass spectrum of 3-BACZ.

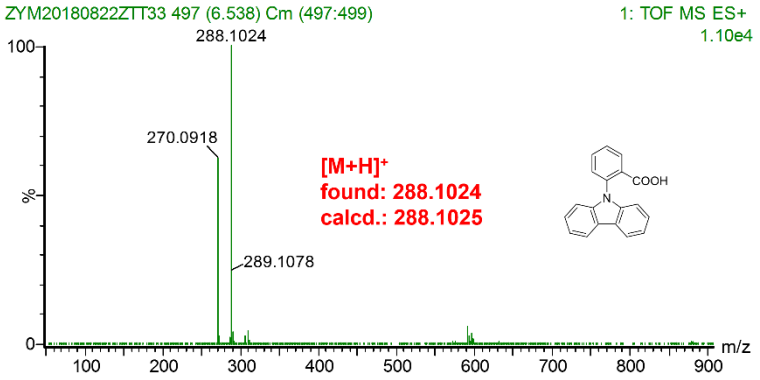

Fig. S3 High resolution mass spectrum of 2-BACZ.

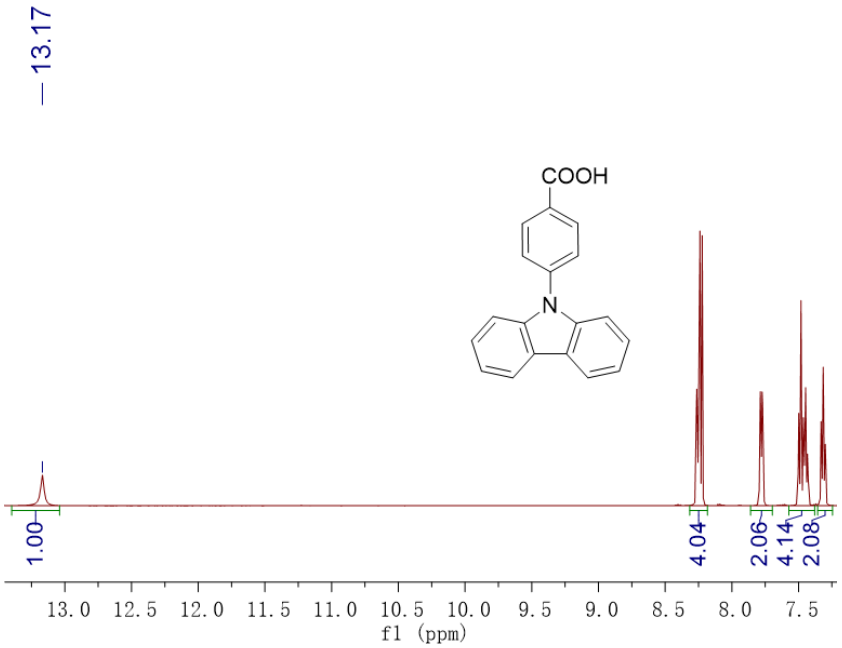

Fig. S4 ^{1}H NMR spectrum of 4-BACZ in DMSO-d_6.

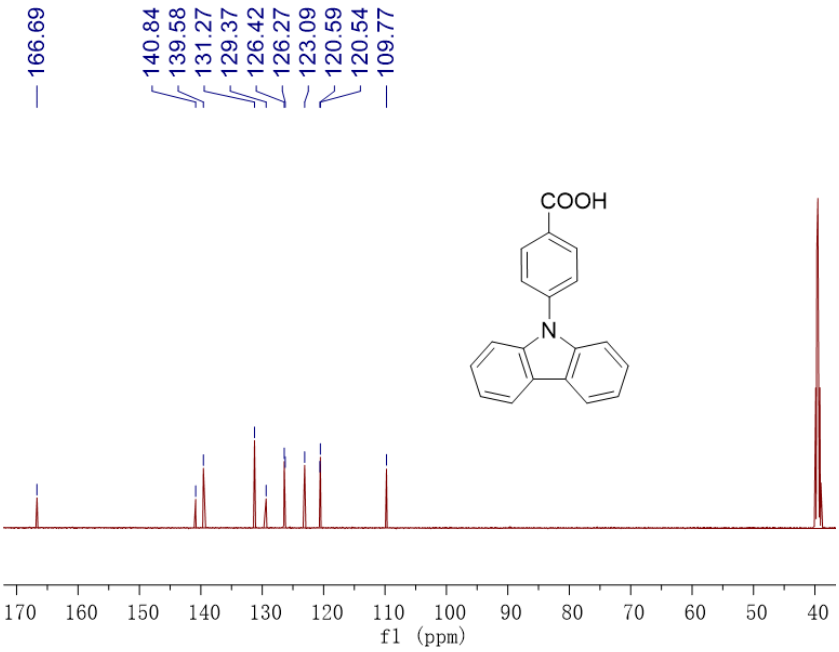

Fig. S5 ^{13}C NMR spectrum of 4-BACZ in DMSO-d_6.

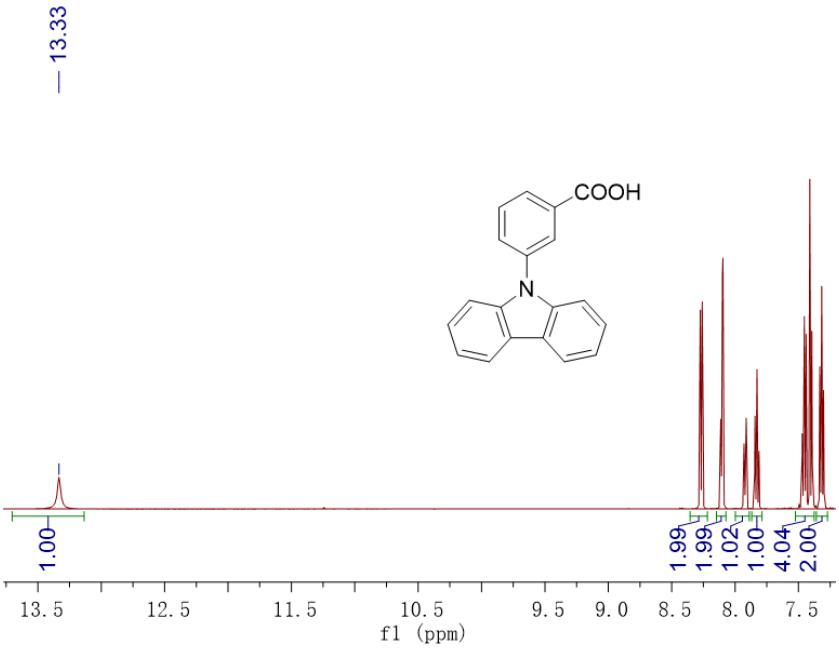

Fig. S6 ^{1}H NMR spectrum of 3-BACZ in DMSO-d_6.

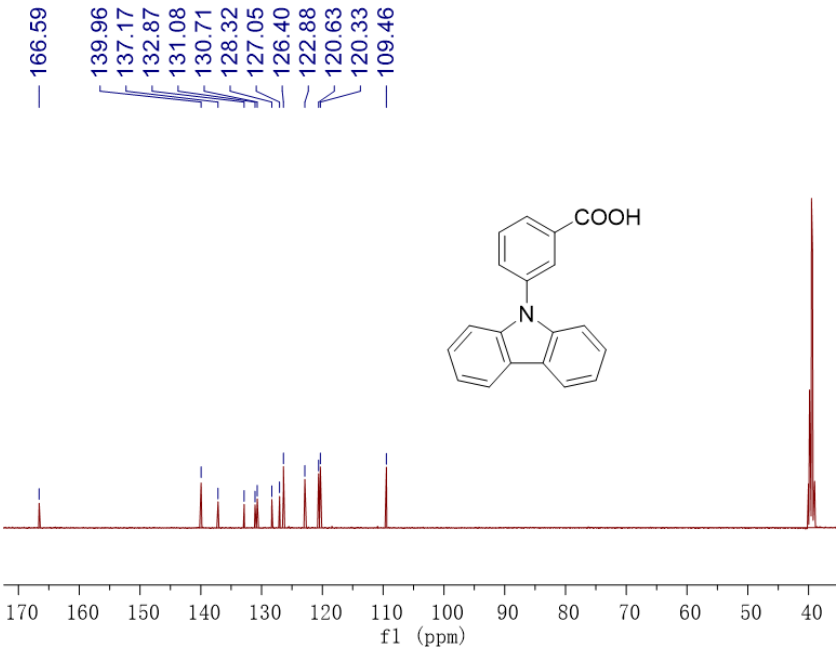

Fig. S7 ^{13}C NMR spectrum of 3-BACZ in DMSO-d_6.

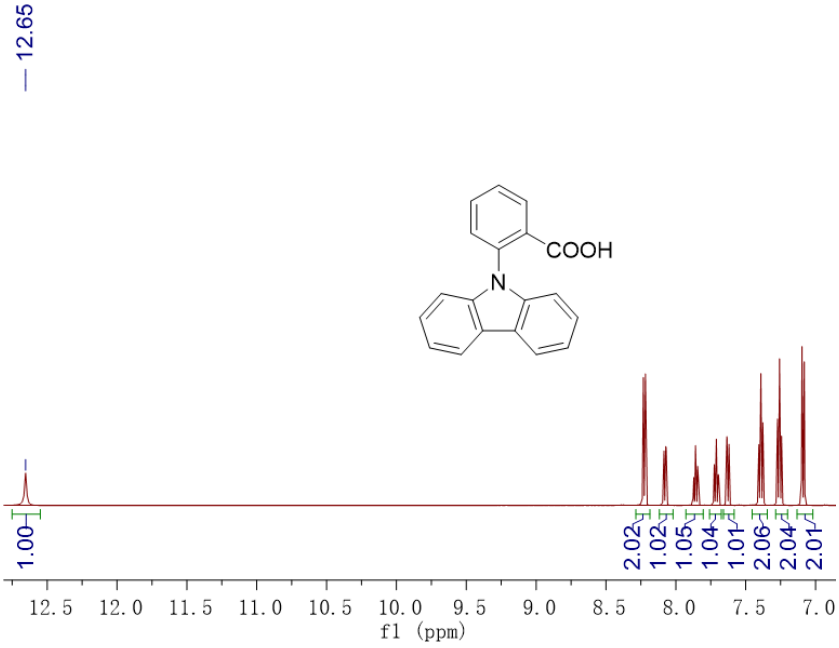

Fig. S8 ^{1}H NMR spectrum of 2-BACZ in DMSO-d_6.

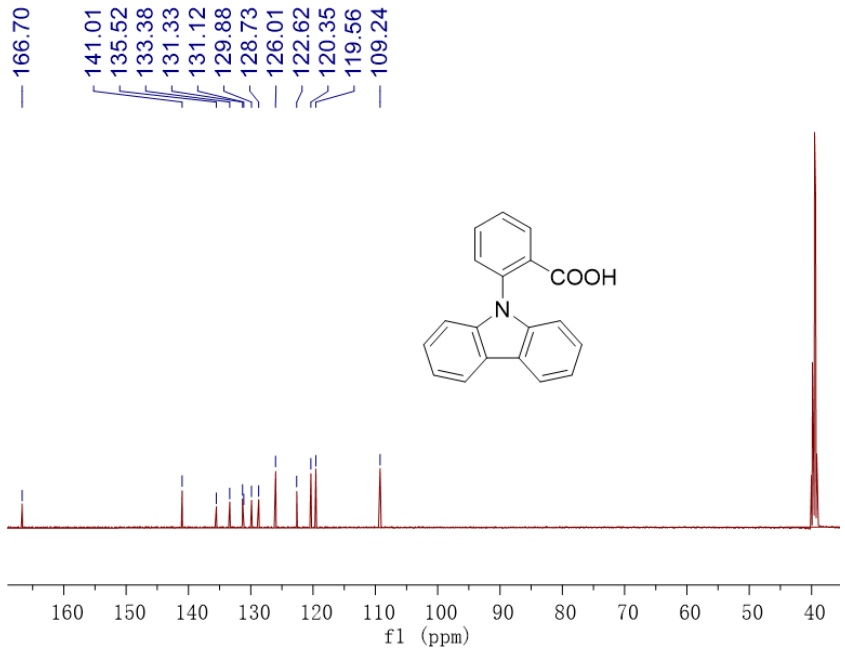

Fig. S9 ^{13}C NMR spectrum of 2-BACZ in DMSO-d_6.

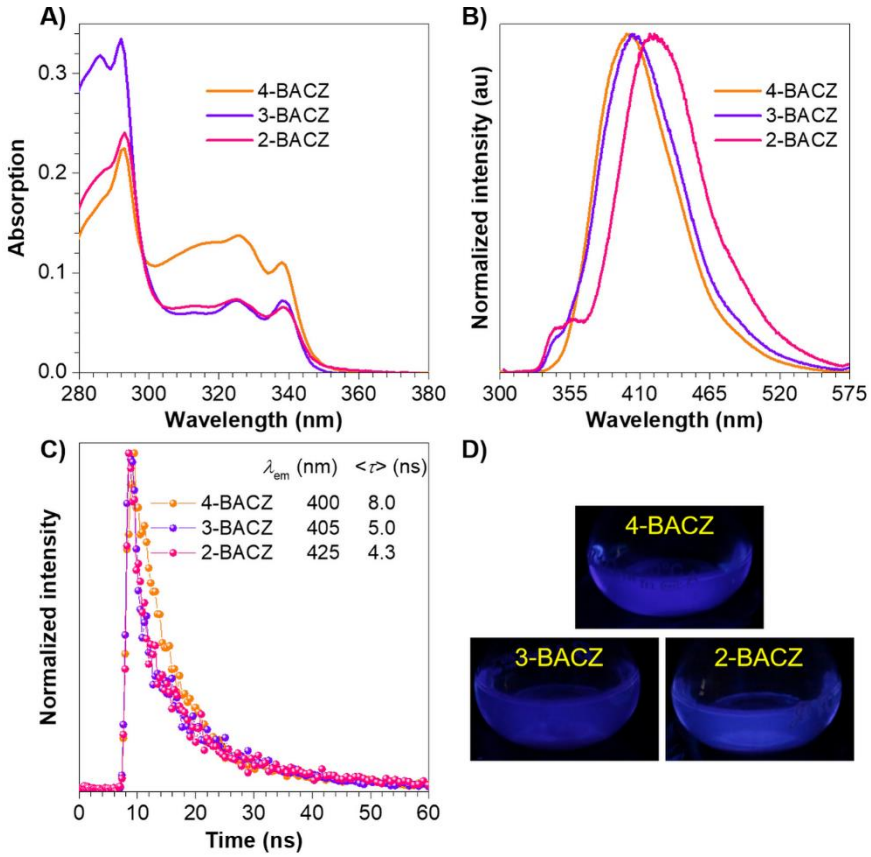

Fig. S10 (A) Absorption, (B) emission (λ_{ex} = 293 nm), (C) lifetime (λ_{ex} = 325 nm) and (D) photos taken under 312 nm UV of 4-BACZ, 3-BACZ and 2-BACZ in THF solution (10^{-5} M).

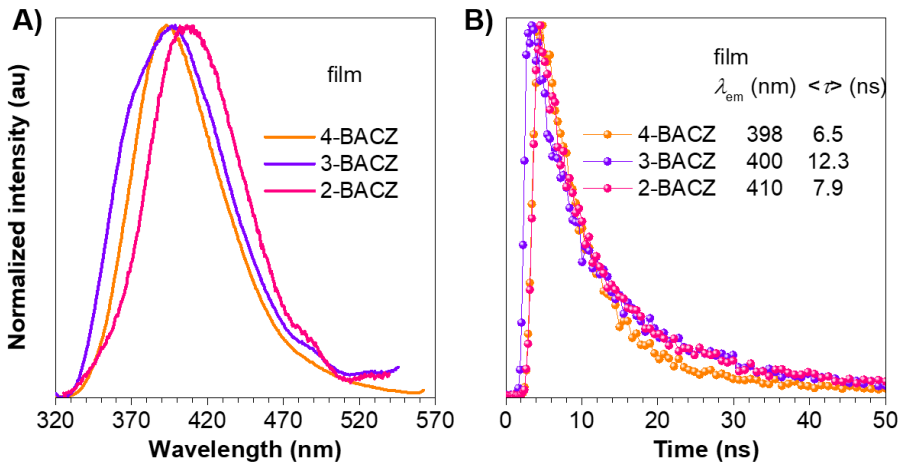

Fig. S11 (A) Emission spectra (λ_{ex} = 293 nm) and (B) lifetimes (λ_{ex} = 335 nm) of the films with 1 wt% compounds for 4-BACZ, 3-BACZ and 2-BACZ.

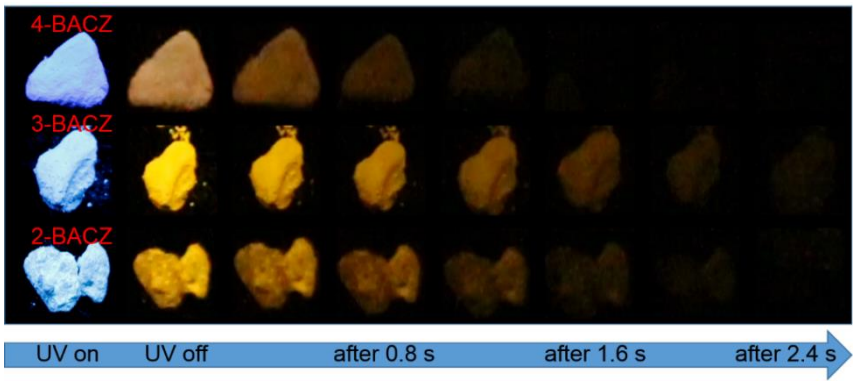

Fig. S12 Photographs of 4-BACZ, 3-BACZ and 2-BACZ solids taken before and after ceasing 365 nm UV light.

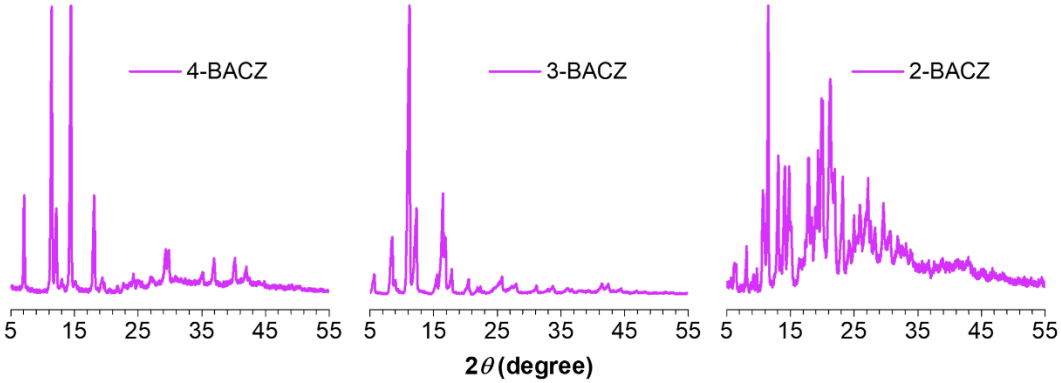

Fig. S13 XRD patterns of the 4-BACZ, 3-BACZ and 2-BACZ solids.

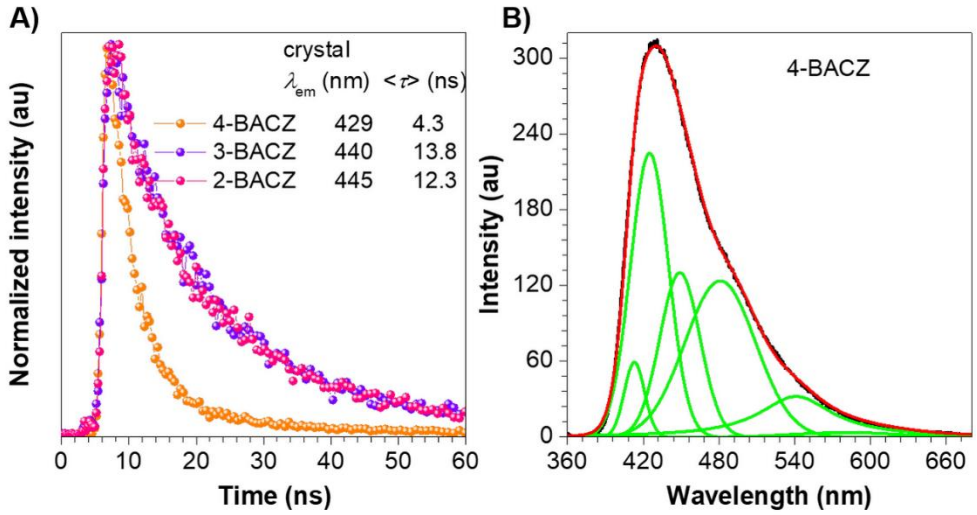

Fig. S14 (A) Fluorescence lifetimes for 4-BACZ, 3-BACZ, and 2-BACZ crystals and (B) peak deconvolution analysis curves for 4-BACZ.

The RTP yields (Φ_p) were calculated based on their proportions of the area of RTP peaks in the whole emissions. For 4-BACZ: $\Phi_p = 53.26\% \times \frac{397.57+3105.64}{397.57+3105.64+8699.93+5200.00+8499.93+1200.00} \approx 6.9\%$ (Table S1).

Table S1 The peaks fitting data for 4-BACZ.

Peak index	Peak type	Area Intg	FWHM	Max height	Center Grvty	Area IntgP
1	Gaussian	0.00	0.00	0.00	397.36	0.00
2	Gaussian	1200.00	19.00	59.33	413.00	4.43
3	Gaussian	8499.93	35.50	224.94	425.00	31.36
4	Gaussian	5200.00	37.50	130.27	449.00	19.19
5	Gaussian	8699.93	66.00	123.83	481.00	32.10
6	Lorentz	3105.64	71.00	32.28	541.00	11.46
7	Gaussian	397.57	100.00	3.76	581.00	1.47

Table S2 Single crystal data of 4-BACZ, 3-BACZ and 2-BACZ.

Compound reference	4-BACZ	3-BACZ	2-BACZ
Chemical formula	$C_{19}H_{13}NO_2$	$C_{19}H_{13}NO_2$	$C_{19}H_{13}NO_2$
Formula Mass	287.30	287.30	287.30
system	Triclinic	Monoclinic	Monoclinic
a/Å	11.660(2)	4.02120(10)	27.6342(16)
b/Å	15.654(4)	18.6170(4)	8.7182(5)
c/Å	18.325(4)	20.8228(5)	12.6486(7)
α/°	88.065	90	90
β/°	75.24(2)	94.2040(10)	101.026(2)
γ/°	68.408	90	90
Unit cell volume/Å^3	3000.7(12)	1554.66(6)	2991.1(3)
Temperature/K	299	299	298
Space group	P -1	P 21/c	P 21/c
Density/(g cm^{-3})	1.272	1.227	1.276
c	8	4	4

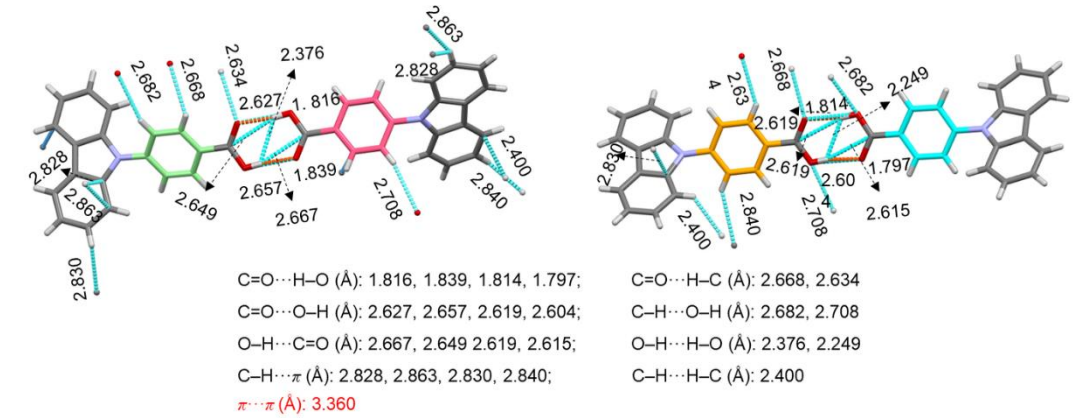

Fig. S15 All intramolecular contacts of 4-BACZ in single crystal structure.

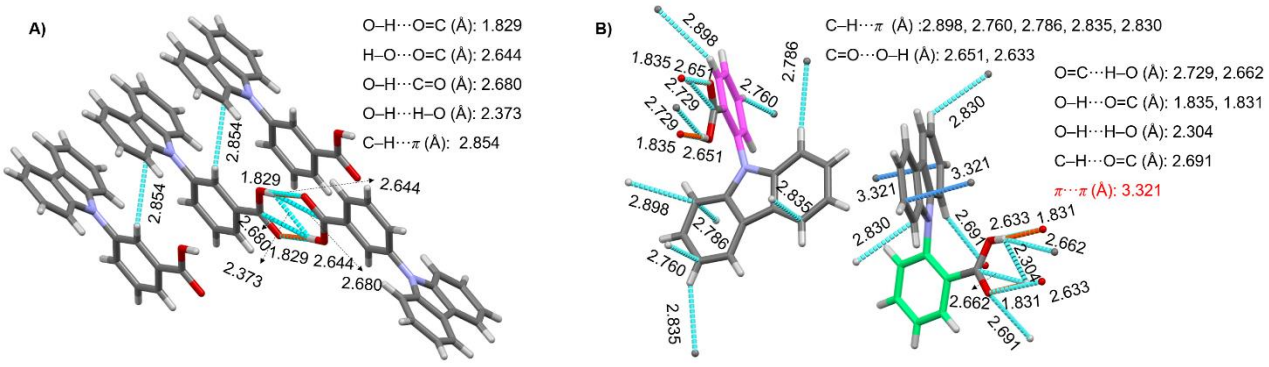

Fig. S16 All intramolecular contacts of (A) 3-BACZ and (B) 2-BACZ in single crystal structure.

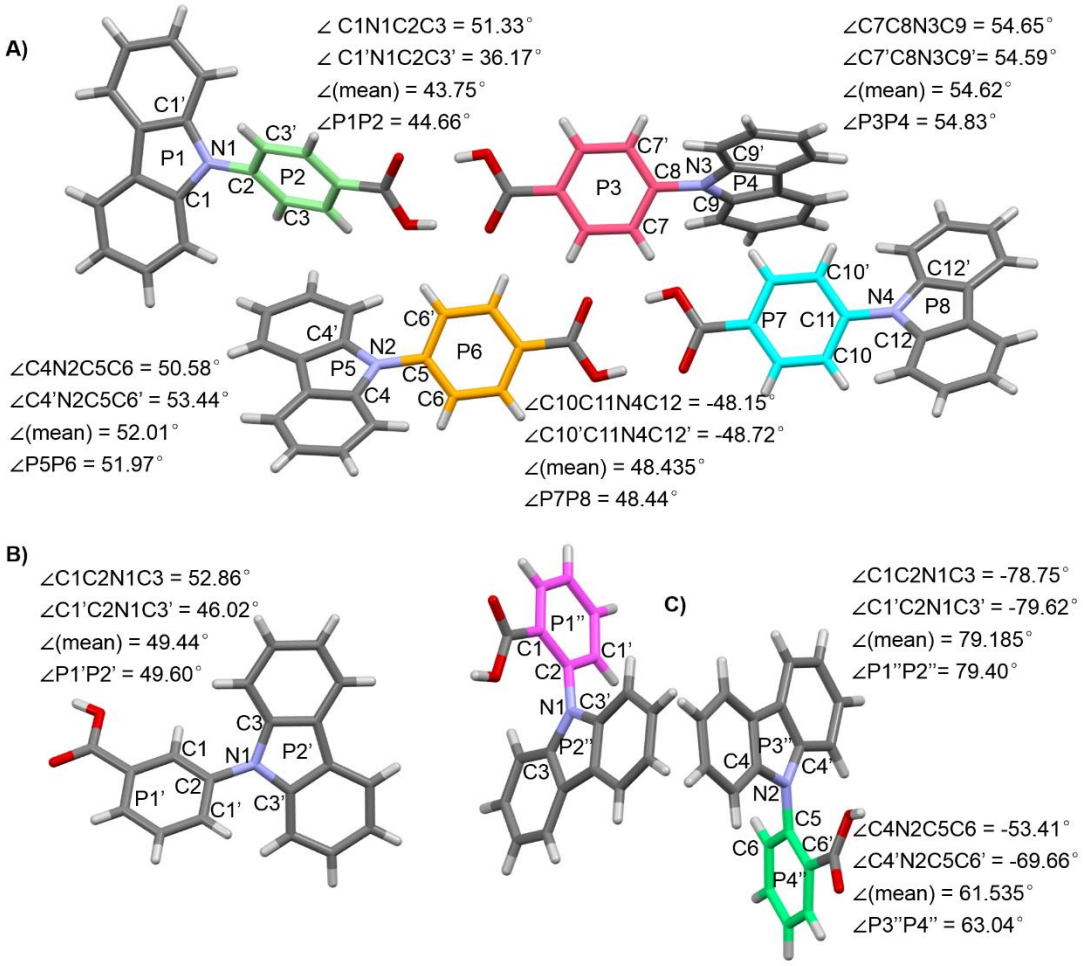

Fig. S17 Torsion angles between CZ and benzene ring (BR) of (A) 4-BACZ, (B) 3-BACZ and (C) 2-BACZ.

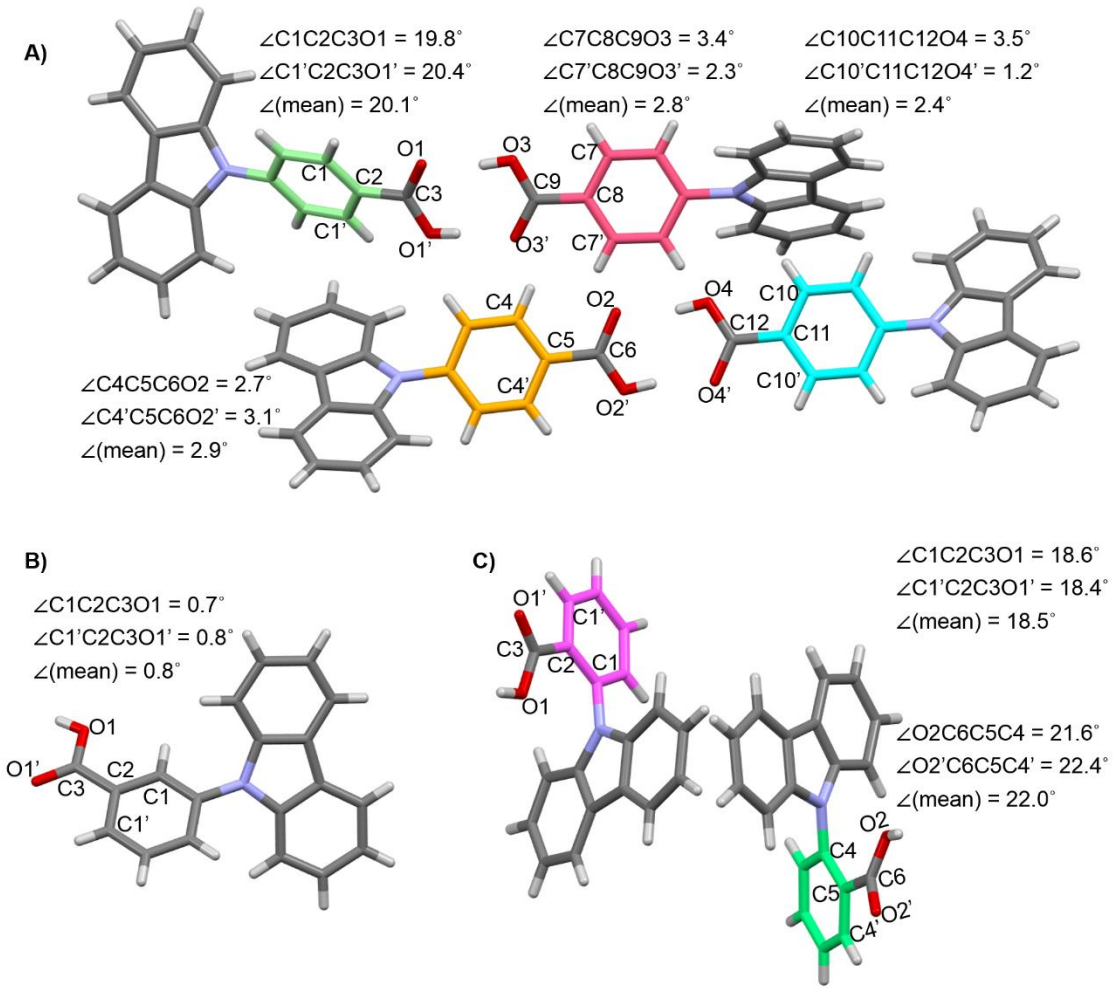

Fig. S18 Torsion angles between carboxyl and BR of (A) 4-BACZ, (B) 3-BACZ and (C) 2-BACZ.

Table S3 Torsion angle between CZ and BR of 4-BACZ, 3-BACZ and 2-BACZ.

compounds	torsion angle between CZ and BR/°	mean torsion angle/°	mean (mean torsion angle)/°
4-BACZ	51.3/36.2	43.8	49.7
	50.6/53.4	52.0	
	54.7/54.6	54.6	
3-BACZ	48.2/48.7	48.4	
	52.9/46.0	49.4	
2-BACZ	78.8/79.6	79.2	70.4
	53.4/69.7	61.5	

Table S4 Torsion angle between carboxyl and BR of 4-BACZ, 3-BACZ and 2-BACZ.

compounds	torsion angle between carboxyl and BR/°	mean torsion angle/°	mean (mean torsion angle)/°
4-BACZ	19.8/20.4	20.1	7.05
	3.4/2.3	2.8	
	3.5/1.2	2.4	
3-BACZ	2.7/3.1	2.9	
	0.7/0.8	0.8	
2-BACZ	18.6/18.4	18.5	20.3
	21.6/22.4	22.0	

Table S5 Torsion angle between CZ and BR of 4-MBACZ, 3-MBACZ and 2-MBACZ.[a]

compounds	torsion angle between CZ and BR/°	mean torsion angle/°	mean (mean torsion angle)/°
4-MBACZ	55.6/48.3	52.0	71.5
3-MBACZ	43.7/52.0	47.9	
2-MBACZ	79.8/82.2	81.0	
	61.4/62.6	62.0	
	79.0/80.6	79.8	
	63.6/62.6	63.1	

[a] Data of 4-MBACZ, 3-MBACZ and 2-MBACZ were adopted from our report [S1].

Table S6 Torsion angle between carboxyl and BR of 4-MBACZ, 3-MBACZ and 2-MBACZ.[a]

compounds	torsion angle between carboxyl and BR/°	mean torsion angle/°	mean (mean torsion angle)/°
4-MBACZ	6.6/5.9	6.3	29.1
3-MBACZ	7.3/7.8	7.5	
2-MBACZ	20.5/21.2	20.8	
	39.4/38.7	39.1	
	36.0/38.1	37.1	
	19.6/19.4	19.5	

[a] Data of 4-MBACZ, 3-MBACZ and 2-MBACZ were adopted from our report [S1].

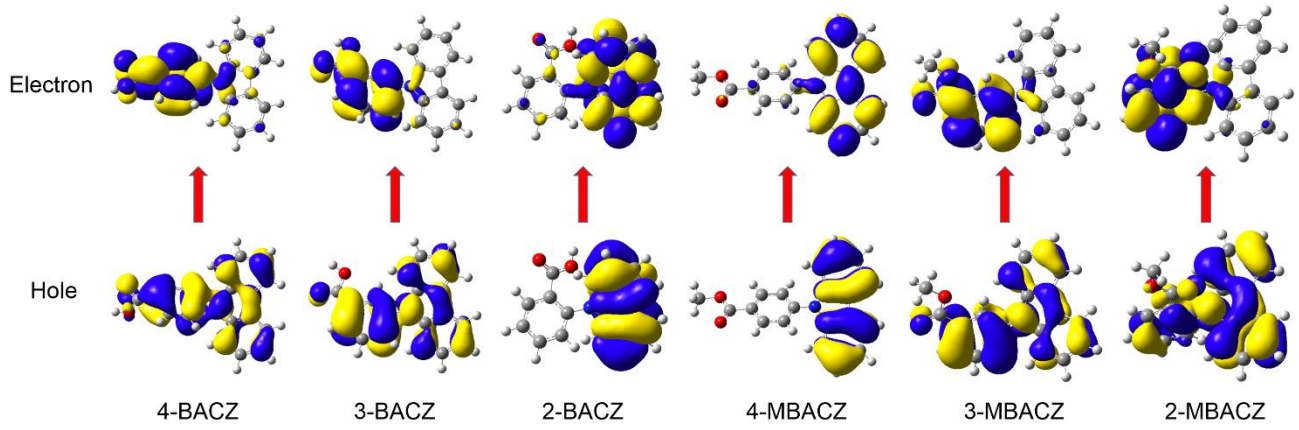

Fig. S19 The natural transition orbitals (NTOs) of T_1 states of 4-BACZ, 3-BACZ, 2-BACZ, 4-MBACZ, 3-MBACZ and 2-MBACZ.

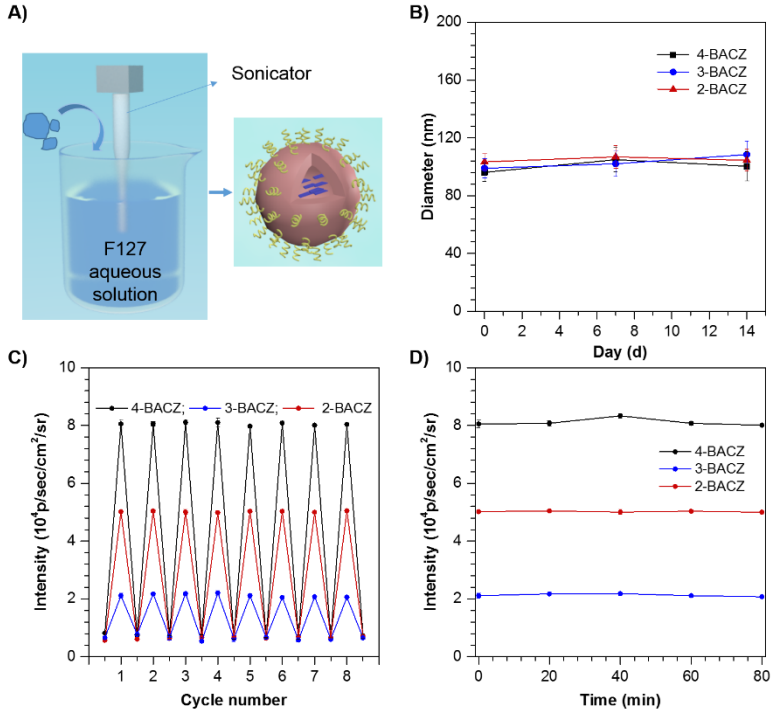

Fig. S20 (A) Preparation of nanoparticles and schematic diagram of nanoparticles. (B) The diameters of 4-BACZ, 3-BACZ and 2-BACZ NPs after storage at 4 °C in dark for 6 and 14 days respectively. (C) The phosphorescence intensities of 4-BACZ, 3-BACZ, 2-BACZ NPs solutions as a function of the cycle number of light activation. (D) The ultralong phosphorescence intensities of 4-BACZ, 3-BACZ and 2-BACZ NPs under continuous light irradiation for 80 min (the power density: 10 mW cm^{-2}).

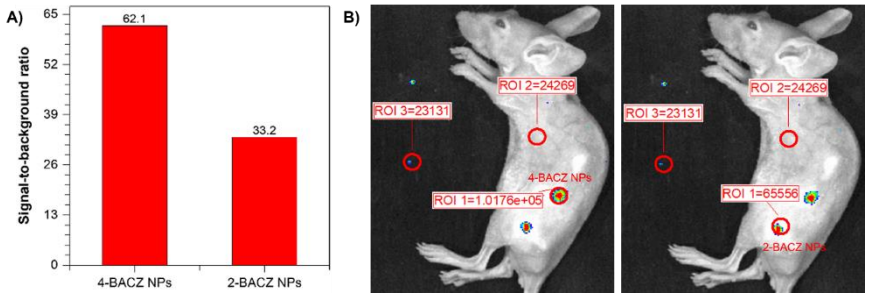

Fig. S21 (A) Signal-to-background ratio (SBR) of 4-BACZ NPs and 2-BACZ NPs for in vivo imaging; (B) the SBR calculation diagram of (left) 4-BACZ and (right) 2-BACZ NPs. It was calculated according to the previous reference [S4]. SBR = $\frac{(\text{RTP signal, ROI 1})-(\text{background 2, ROI 3})}{(\text{background 1, ROI 2})-(\text{background 2, ROI 3})}$

References

[S1] T. Zhang, X. Wang, Z. An, Z. Fang, Y. Zhang and W. Z. Yuan, *ChemPhysChem*, 2018, **19**, 2389.

[S2] L. M. Lifshits, B. C. Noll and J. K. Klosterman, *ChemComm,* 2015, **51**, 11603.

[S3] M. J. Frisch, G. W. Trucks, H. B. Schlegel, G. E. Scuseria, M. A. Robb, J. R. Cheeseman, G. Scalmani, V. Barone, B. Mennucci, G. A. Petersson, H. Nakatsuji, M. Caricato, X. Li, H. P. Hratchian, A. F. Izmaylov, J. Bloino, G. Zheng, J. L. Sonnenberg, M. Hada, M. Ehara, K. Toyota, R. Fukuda, J. Hasegawa, M. Ishida, T. Nakajima, Y. Honda, O. Kitao, H. Nakai, T. Vreven, Jr. J. A. Montgomery, J. E. Peralta, F. Ogliaro, M. J. Bearpark, J. Heyd, E. N. Brothers, K. N. Kudin, V. N. Staroverov, R. Kobayashi, J. Normand, K. Raghavachari, A. P. Rendell, J. C. Burant, S. S. Iyengar, J. Tomasi, M. Cossi, N. Rega, N. J. Millam, M. Klene, J. E. Knox, J. B. Cross, V. Bakken, C. Adamo, J. Jaramillo, R. Gomperts, R. E. Stratmann, O. Yazyev, A. J. Austin, R. Cammi, C. Pomelli, J. W. Ochterski, R. L. Martin, K. Morokuma, V. G. Zakrzewski, G. A. Voth, P. Salvador, J. J. Dannenberg, S. Dapprich, A. D. Daniels, Farkas, J. B. Foresman, J. V. Ortiz, J. Cioslowski and D. J. Fox, Gaussian, Inc.: Wallingford, CT, USA, 2009.

[S4] Q. Miao, C. Xie, X. Zhen, Y. Lyu, H. Duan, X. Liu, J. V. Jokerst and K. Pu, Nat. Biotechnol, 2017, *35*, 1102.